A Random Pore Model for Fluid-Solid Reactions:

II. Diffusion and Transport Effects

S. K. BHATIA
and
D. D. PERLMUTTER
Department of Chemical Engineering
University of Pennsylvania
Philadelphia, Pennsylvania 19104

The prior random pore model for kinetically controlled fluid-solid reaction (Bhatia and Perlmutter, 1980) is generalized to include transport effects arising from boundary layer, intraparticle, and product layer diffusion. Numerical solutions are presented for a variety of conditions. The results show that the rate and surface area maxima predicted in the kinetic regime are shifted to lower conversions as intraparticle or product layer diffusional resistances increase. In addition, with increasing temperature a decrease in the overall reaction surface is predicted, in agreement with experimental findings (Kawahata and Walker, 1962).

For reactions accompanied by an increase in the volume of the solid phase, it is shown that incomplete conversion may be expected, the ultimate conversion decreasing with an increase in the intrapellet diffusional resistance. Optimal temperatures for such reactions are also identified.

SCOPE

A model is presented which incorporates diffusional effects into the random pore model (Bhatia and Perlmutter, 1980) for kinetically controlled fluid solid reactions. The model is formulated in terms of generalized pore size distributions, without the uniform-size idealizations inherent in earlier models for grain reactions (Szekely and Evans, 1979; Calvelo and Smith, 1971), or pore reactions (Petersen, 1957; Ramachandran and Smith, 1977). It is shown that the previously established correspondence with the grain model exists as well when moderate transport resistances are included.

The model considers the reaction-produced structural modifications associated with the change in the volume of the solid phase. The model predictions are consistent with the experimentally observed temperature optima that occur when the solid phase increases in volume (Hartman and Coughlin, 1976).

CONCLUSIONS AND SIGNIFICANCE

The generalized random pore model presented here offers a technique for analyzing fluid-solid reactions when transport resistances are significant. For a large enough Thiele modulus, or modified Biot modulus, only rate decreases may be expected, even for those pore structures that show rate maxima when diffusional processes are rapid. In the absence of a solid product the model predicts that when temperature is raised, increasing diffusional resistance decreases the surface area developed at any conversion. This suggests that transport effects were important in the experimental study of Kawahata and Walker (1962) who observed this effect.

The model indicates that when there is an increase in volume of the solid phase, and if the initial porosity is not large enough, rapid surface pore closure results in incomplete conversions. The results also show that for such reactions, rapid surface pore closure may play a role in determining the optimal temperature, as noticed by Hartman and Coughlin (1976) for the lime-SO_2 reaction.

In the prior paper of this series (Bhatia and Perlmutter, 1980) the authors presented a random pore model that subsumed several earlier approaches based on either grain or pore structures. The new result considered that the reaction surfaces within the solid arise from the overlapping of a random set of cylinders. When nucleation is rapid in the regime of kinetic control the overall rate of reaction was found to be:

$$\frac{dX}{dt} = \frac{k_s C^n S_o (1 - X)\sqrt{1 - \psi \ln (1 - X)}}{(1 - \epsilon_o)} \tag{1}$$

and it was shown that this relationship is in agreement with the Petersen (1957) model over most of the conversion range, when structural parameters are chosen to be consistent with the restrictions of Petersen's assumptions. Furthermore, by comparison of Eq. 1 with the rate expression derived from a grain model:

$$\frac{dX}{dt} = \frac{k_s C^n S_o (1 - X)^m}{(1 - \epsilon_o)} \tag{2}$$

the close linkage was demonstrated between the effective grain shape parameter m and the pore structure parameter ψ.

In this paper the model for kinetic control (Bhatia and Perlmutter, 1980) is generalized to include: (i) external mass transfer, (ii) intraparticle diffusion, and (iii) product layer diffusion. Any one or all of these transport resistances may be significant or dominant, depending on the particle size, tempera-

S. K. Bhatia is with Mobil Research and Development Corp., Paulsboro, N.J. 08066.
Part I of this paper appeared in *AIChE J.*, **26**, 379 (1980).

0001-1541-81-4365-0247-$2.00.

(a) (b) (c)

Figure 1. Development of reaction surface. The blackened area represents unreacted solid B, the dotted area the product layer. (a) Early stage, showing product layer around each pore; (b) Intermediate stage, showing some overlapping reaction surfaces; (c) Later stage, showing full development of the product layer and the reaction surface for the particular view chosen.

ture, and the structural properties of the solid.

A general representation for irreversible reaction and diffusion in a spherical particle with no bulk flow is:

$$\frac{1}{R^2}\frac{\partial}{\partial R}\left(D_e R^2 \frac{\partial C}{\partial R}\right) = \frac{a\rho(1-\epsilon_o)}{Mb}\frac{dX}{dt} \tag{3}$$

where, following Luss (1968) and Bischoff (1963), the pseudo-steady state hypothesis has been invoked. The boundary conditions for Eq. 3 are based on radial symmetry, and on an external boundary layer resistance expressed in terms of a mass transfer coefficient:

$$\frac{\partial C}{\partial R} = 0 \quad \text{at } R = 0 \tag{4}$$

and,

$$D_e \frac{\partial C}{\partial R} = k_m(C_b - C) \quad \text{at } R = R_o \tag{5}$$

In general the effective diffusivity will vary with the structural parameters of the solid in the form:

$$D_e = D\frac{\epsilon}{\gamma(\epsilon)} \tag{6}$$

where $\gamma(\epsilon)$ is the tortuosity of the solid, usually in the range of 1.5 to 2 (Satterfield, 1970; Smith, 1970). According to the model of Wakao and Smith (1963):

$$\gamma(\epsilon) = \frac{1}{\epsilon} \tag{7}$$

suggesting that tortuosity varies as reaction proceeds, even though some researchers have treated γ as invariant during the reaction process (Hartman and Coughlin, 1976).

MODEL DEVELOPMENT

Consider the irreversible reaction of a spherical particle of solid B with fluid A, according to the stoichiometry:

$$a\mathrm{A(g)} + b\mathrm{B(s)} \rightarrow p\mathrm{P(g)} + q\mathrm{Q(s)} \tag{8}$$

The solid is relatively macroporous; if they are present at all, micropores have an effectiveness factor of unity. Reaction is initiated on pore boundaries resulting in a set of growing surfaces at each radial position within the particle. The product Q accumulates in the space between the growing reaction surfaces and the pore boundaries offering a diffusional resistance to the flow of fluid A. As reaction proceeds it is inevitable that neighboring surfaces will eventually intersect, with an accompanying loss in area.

Following the arguments cited (Bhatia and Perlmutter, 1980) consider the reaction surface to be the result of the random overlapping of a set of cylindrical surfaces of size distribution $f(r)$, where $f(r)dr$ is the total length of the cylindrical surfaces, per unit volume of space, having radii between r and $r + dr$. A balance over the size distribution of the growing cylinders at any radial position yields

$$\frac{\partial f}{\partial t} + \frac{\partial}{\partial r}\left(f\frac{dr}{dt}\right) = 0 \tag{9}$$

If the rate of reaction is first order with respect to reactant A and proportional to surface area:

$$\frac{dr}{dt} = k_s C_i \tag{10}$$

and

$$\frac{dV}{dt} = k_s C_i S \tag{11}$$

where C_i is the concentration of fluid reactant A, assumed to be uniform over the entire reaction surface at any radial position within the pellet. It should be noted that the total length of the cylindrical system L_E, the surface area S_E, and the volume V_E which were defined in Part I (Eqs. 8 to 10) are applicable to the problem at hand and produce an identical result for the reaction rate, but with the bulk concentration C replaced for this case by C_i:

$$\frac{dX}{dt} = \frac{k_s S_o C_i}{(1-\epsilon_o)}(1-X)\sqrt{1-\psi\ln(1-X)} \tag{12}$$

It remains to relate the interfacial concentration C_i to the concentration in the pores at any radial position in the pellet.

To this end consider the two-dimensional projection shown in Figure 1 of a microregion at some radical position of the solid in each of three stages of development: (a) an early stage in which the reaction surfaces have formed around each pore; (b) an intermediate stage in which some of the reaction surfaces have intersected; (c) a later stage in which all of the surfaces in that micro-region have intersected.

In each case the space between the pore surfaces and the reaction surface is filled with reaction product through which the fluid A must diffuse. It should be noted that the pores and the reaction surfaces associated with them are not necessarily parallel, but can have any orientation in three dimensional space. Thus, although no pore intersections are depicted in Figure 1, the pore system actually forms a single overlapping network with a closed surface. With increasing conversion a reaction surface develops, growing from the initial pore system surface. It is assumed that the reaction surface grows normal to itself, so that any point on its boundary traces a non-planar curve in three dimensions.

Measured along this curve the diffusion distance for reactant A is then the distance separating the reaction surface from the surface of the pores closest to it. Thus, in Figure 1(C) the diffusion thickness is the distance between the reaction surface and the dashed curve representing the periphery of the nearest pores. Inside the dashed curve the concentration of fluid A is small since all the pores shown, being at the same radial position in the particle, contain fluid having the same concentration.

Because the ratio of volume of product formed to the volume of solid reacted is Z,

$$V - \epsilon = Z(V - V_o) \tag{13}$$

combining Eqs. 11 and 13 gives the rate of formation of product as a result of reaction as:

$$\frac{d(V - \epsilon)}{dt} = Zk_sC_iS \tag{14}$$

Denoting Δ as the mean thickness of the diffusion layer, and considering it to be small in comparison to the dimensions of the reaction surface:

$$\frac{d\Delta}{dt} = \frac{1}{S}\frac{d(V - \epsilon)}{dt} \tag{15}$$

Combining Eqs. 14 and 15 results in

$$\frac{d\Delta}{dt} = Zk_sC_i \tag{16}$$

Eqs. 12 and 16 provide:

$$\frac{d\Delta}{dX} = \frac{Z(1 - \epsilon_o)}{S_o(1 - X)\sqrt{1 - \psi \ln (1 - X)}} \tag{17}$$

which, upon integration with the initial condition $\Delta = 0$ when $X = 0$, yields

$$\Delta = \frac{2Z(1 - \epsilon_o)}{\psi S_o}\left[\sqrt{1 - \psi \ln (1 - X)} - 1\right] \tag{18}$$

as the effective local thickness of the diffusion layer, at any local conversion X. Assuming a linear concentration gradient of the species A, in the diffusion layer of thickness Δ, a material balance over A provides:

$$D_P\frac{C - C_i}{\Delta} = \frac{k_sC_ia\rho}{Mb} \tag{19}$$

Combining Eqs. 12, 18, and 19 yields an expression for the local reaction rate:

$$\frac{dX}{dt} = \frac{k_sS_oC(1 - X)\sqrt{1 - \psi \ln (1 - X)}}{(1 - \epsilon_o)\left[1 + \frac{\beta Z}{\psi}\left(\sqrt{1 - \psi \ln (1 - X)} - 1\right)\right]} \tag{20}$$

where the parameter β is a modified Biot modulus. The conversion time behavior of a porous pellet of solid B may be obtained by the simultaneous solution of Eqs. 3 to 5 and 20. In dimensionless form these equations become:

$$\frac{1}{\eta^2}\frac{\partial}{\partial \eta}\left(D_e^*\eta^2\frac{\partial C^*}{\partial \eta}\right) = \phi^2\frac{dX}{d\tau} \tag{21}$$

and

$$\frac{dX}{d\tau} = \frac{C^*(1 - X)\sqrt{1 - \psi \ln (1 - X)}}{1 + \frac{\beta Z}{\psi}\left[\sqrt{1 - \psi \ln (1 - X)} - 1\right]} \tag{22}$$

with boundary conditions

$$\frac{\partial C^*}{\partial \eta} = 0 \quad \text{at } \eta = 0$$

$$\frac{\partial C^*}{\partial \eta} = \frac{Sh(1 - C^*)}{D_e^*} \quad \text{at } \eta = 1 \tag{23}$$

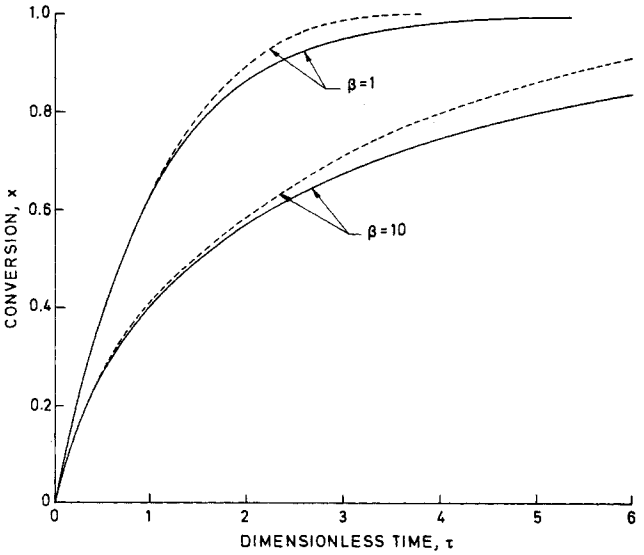

Figure 2. Comparison of conversion-time behavior predicted by the random-pore model and the grain model, when effects of chemical reaction and product layer diffusion dominate. The solid lines are from the random pore model with $\psi = 1$. The dashed curves are from the spherical grain model. In all cases $Z = 1$.

and the initial condition

$$X = 0 \quad \text{at } \tau = 0, \quad \text{for } 0 \le \eta \le 1 \tag{24}$$

The effective diffusivity varies with conversion according to the representation in Eq. 6 so that

$$D_e^* = \frac{\epsilon^*\gamma(\epsilon_o)}{\gamma(\epsilon)} \tag{25}$$

Allowing for porosity change with reaction:

$$\epsilon^* = 1 - \frac{(Z - 1)(1 - \epsilon_o)X}{\epsilon_o} \tag{26}$$

RESULTS AND DISCUSSION

Equations 21-26 were solved numerically using an orthogonal collocation technique based on the Legendre polynomials (Finlayson, 1972) to transform Eq. 21 into a system of linear algebraic equations. Eq. 22 was simultaneously integrated using a Runga-Kutta technique. It was found that, in the range of pa-

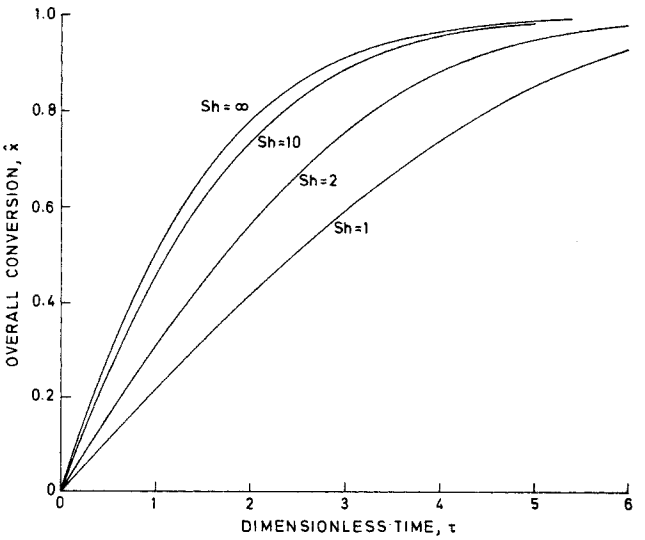

Figure 3. Effect of Sherwood Number on conversion-time behavior. Parameters are: $\phi = 3$, $\psi = \beta = Z = 1$.

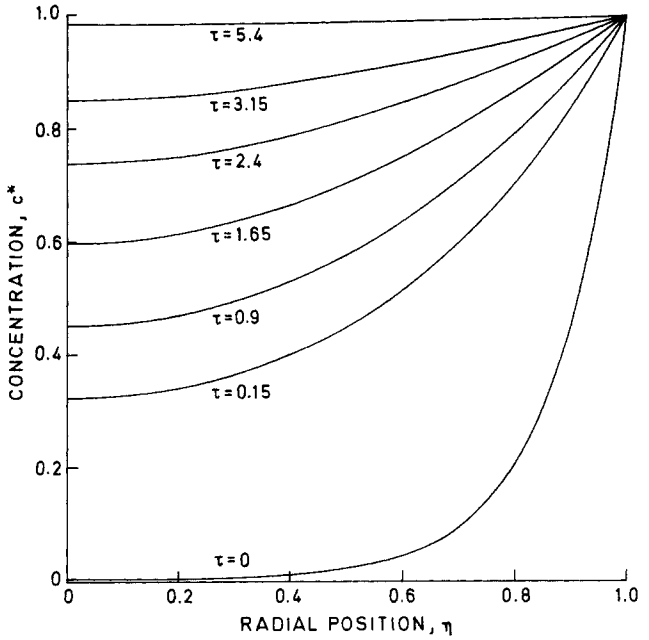

Figure 4. Concentration profiles of fluid reactant A at various values of dimensionless time. Parameters are: $\psi = 3$, $Sh = \infty$, $\psi = \beta = Z = 1$.

rameters used, satisfactory convergence occurred with eight or less collocation points.

In the following sections these results are presented for the case of negligible intrapellet diffusional resistance, and for the case in which all diffusional resistances are considered. Unless otherwise specified, the Wakao-Smith model (cf. Eq. 7) was used to account for the variations in effective diffusivity with porosity.

Conversion-Time Behavior

When intrapellet diffusion is rapid, so that chemical kinetics and product layer diffusion control the overall reaction rate, Eq. 22 may be integrated to:

$$X = 1 - \exp\left(\frac{1}{\psi} - \frac{\left[\sqrt{1 + \beta Z\tau} - \left(1 - \frac{\beta Z}{\psi}\right)\right]^2 \psi}{\beta^2 Z^2}\right) \quad (27)$$

The comparable expression for the spherical grain model with $Z = 1$ is, in implicit form (Szekely et al., 1976):

$$\tau = 3[1 - (1 - X)^{1/3}]$$

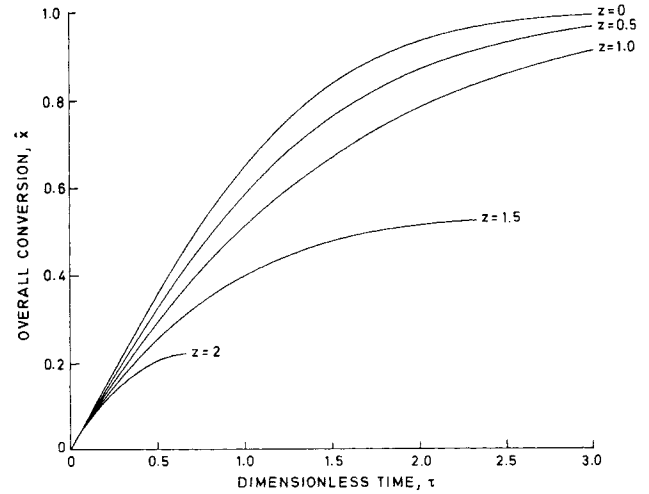

Figure 6. Conversion-time curves for various values of Z. Parameters are: $\phi = 3$, $\epsilon_0 = 0.3$, $Sh = \infty$, $\psi = \beta = 1$.

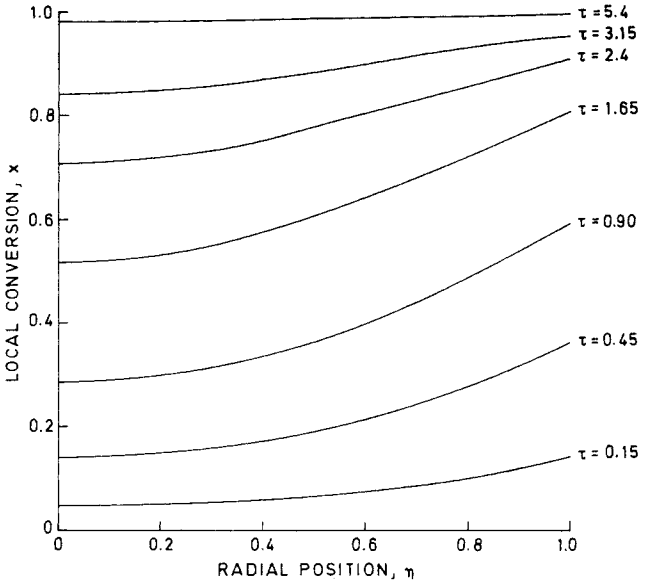

Figure 5. Profiles of local conversion at various values of dimensionless time. Parameters are: $\phi = 3$, $Sh = \infty$, $\psi = \beta = Z = 1$.

$$+ \frac{3\beta}{4}[1 - 3(1 - X)^{2/3} + 2(1 - X)] \quad (28)$$

Figure 2 shows a comparison of the predictions of Eq. 28 with those of Eq. 27 for $Z = 1$ and $\psi = 1$. In general, the agreement is better for smaller values of the modified Biot number, β, and for small conversions. As expected the conversion process is slowed down as the diffusional resistance in the product layer increases, but the results of the random pore model with $\psi = 1$ are nevertheless in close agreement with those of the spherical grain model.

When intraparticle and extraparticle diffusion is considered as well, results are obtained by the simultaneous solution of Eqs. 21 to 26. Figure 3 shows the effect of the external mass transfer resistance in terms of a modified Sherwood number. The overall conversion in Figure 3 was calculated from the Equation:

$$\hat{X} = 3\int_0^1 X\eta^2 d\eta \quad (29)$$

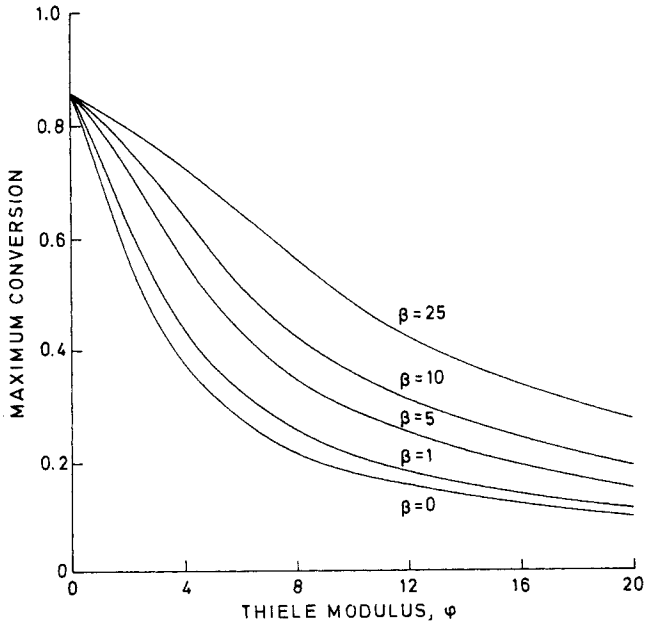

Figure 7. Effect of Thiele Modulus on maximum conversion for various values of β. Parameters are: $\epsilon_0 = 0.3$, $Sh = \infty$, $\psi = 1$, $Z = 1.5$.

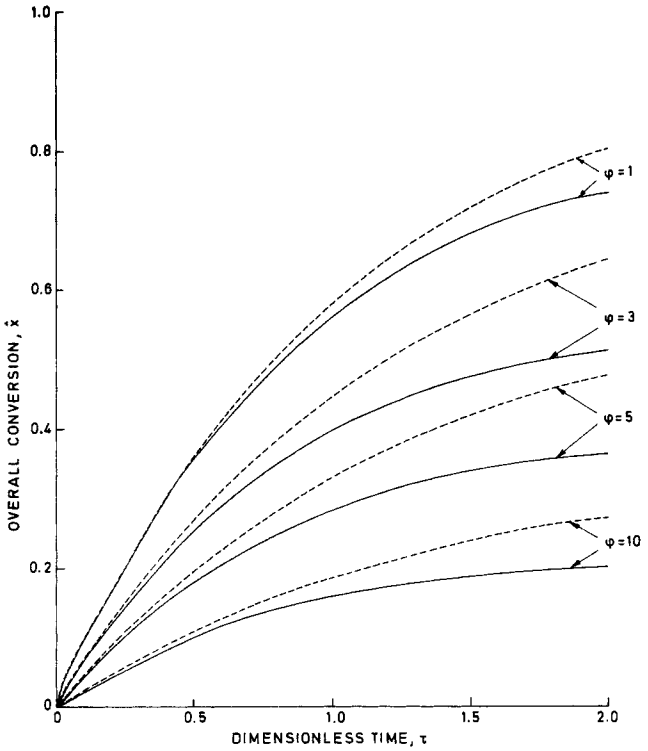

Figure 8. The effect of tortuosity function on conversion for various values of the Thiele Modulus. The solid lines are from the Wakao-Smith (1963) model. The dashed lines are based on a constant tortuosity. Parameters for all cases are: $\epsilon_o = 0.3$, $Sh = \infty$, $\psi = \beta = 1$, $Z = 1.5$.

For the parameter values used the effect of boundary layer diffusion is virtually negligible for values of Sh greater than 10, but it does have a pronounced effect at lower values. The influence of external mass transfer is in all cases more important in the range of intermediate conversions.

Figure 4 shows the concentration profiles within the pellet at various times during the conversion process when boundary layer diffusion is rapid. The profile at $\tau = 0$ is an artifact of the pseudo-steady state hypothesis; had this hypothesis not been used the initial concentration would have been zero everywhere (or any other assumed profile). Nevertheless, as justified by Luss (1968), and Bischoff (1963), the profiles generated using this hypothesis will be achieved very quickly.

With increase in time the profiles flatten out and approach the constant bulk gas concentration. The conversion profiles for the same parameter values are shown in Figure 5. As expected, conversion is initially most rapidly at the surface, where the concentration of the reactant fluid is largest. At later times, however, when the reactant solid close to the surface nears exhaustion, and the concentration profile is flatter, the bulk of the reaction occurs in the interior of the particle.

For some reaction systems (e.g., sulfation of lime by SO_2) the solid product formed occupies a larger volume than the reactant consumed. In such cases, if the initial porosity is low, pore closure may occur and inhibit further reaction prior to complete conversion. In the absence of an intrapellet diffusional resistance Eq. 26 may be used to obtain the conversion at zero porosity:

$$X = \frac{\epsilon_o}{(Z - 1)(1 - \epsilon_o)} \tag{30}$$

When the intrapellet diffusional resistance is appreciable, pore closure will first occur at the surface, stopping further diffusion of the reactant fluid into the particle interior. At this moment the solid may be considered to have attained its maximum conversion, less than that predicted by Eq. 30 which assumes rapid diffusion into the particle. Figure 6 shows conversion-time profiles for a solid with an initial porosity of 0.3, and $\phi = 3$, for various values of the parameter Z.

It may be noted that the reaction stops well before complete conversion is achieved for Z = 1.5 and Z = 2. For Z = 1.5 and $\epsilon_o = 0.3$, for example, Eq. 30 predicts that pore closure will stop further reaction when $X = 0.86$. Because of the presence of a diffusional resistance this value is achieved locally at the surface when only 52 percent conversion is achieved overall. Similarly, for Z = 2 only 22% overall conversion is achieved although the limiting conversion is 43% in the absence of intraparticle gradients.

The effect of the diffusional resistances is more directly shown in Figure 7 which illustrates the dependence of the limiting conversion on the initial Thiele modulus for various values of β. As expected, the maximum conversion decreases with greater intrapellet diffusional resistance. This is also in accord with the experimental results of Hartman and Coughlin (1976) who studied the effect of particle size on the rate of sulfation of lime. The increased conversion at higher levels of β is attributable to the increasing importance of the product layer diffusional resistance resulting in lower intraparticle concentration gradients and allowing greater overall conversion before pore closure occurs at the surface.

In accounting for the variation in effective diffusionty with conversion, the calculations were performed using the Wakao-Smith (1962) Model, which considers the tortuosity as inversely proportional to porosity. If instead the tortuosity is constant as reaction proceeds (Pigford and Sliger, 1973; Hartman and Coughlin, 1976) the model predictions are somewhat modified, as shown in Figure 8. As might be expected, the difference between the two approaches becomes appreciable at the larger values of ϕ. For the parameter values chosen the variation is less than 5% for $\phi \leq 1$.

Development of the Reaction Surface

It was shown in Part I that in the kinetic regime the reaction surface varies with conversion according to:

$$\frac{S}{S_o} = (1 - X)\sqrt{1 - \psi \ln (1 - X)} \tag{31}$$

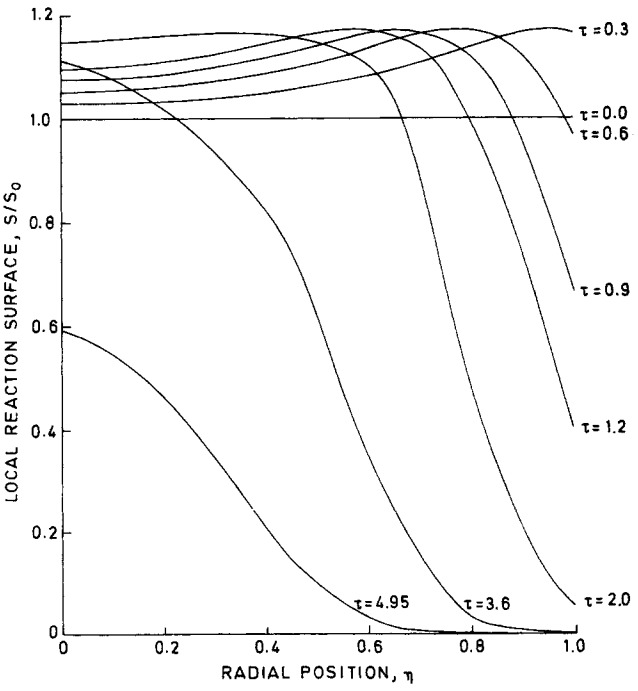

Figure 9. Local reaction surface profiles at various values of dimensionless time. Parameters are: $\phi = 5$, $Sh = \infty$, $\psi = 5$, $\beta = Z = 1$.

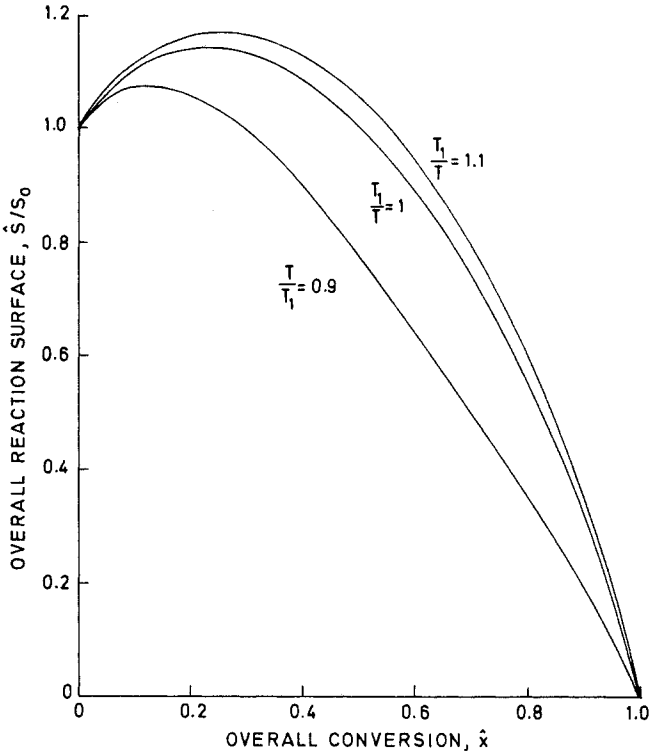

Figure 10. Development of the overall reaction surface with conversion at various reaction temperatures. Parameters are: $\phi = 5$, $\epsilon_o = 0.3$, $Sh = \infty$, $\psi = 5$, $Z = 0$, $e^{\xi/RT_1} = 3.6 \times 10^9$.

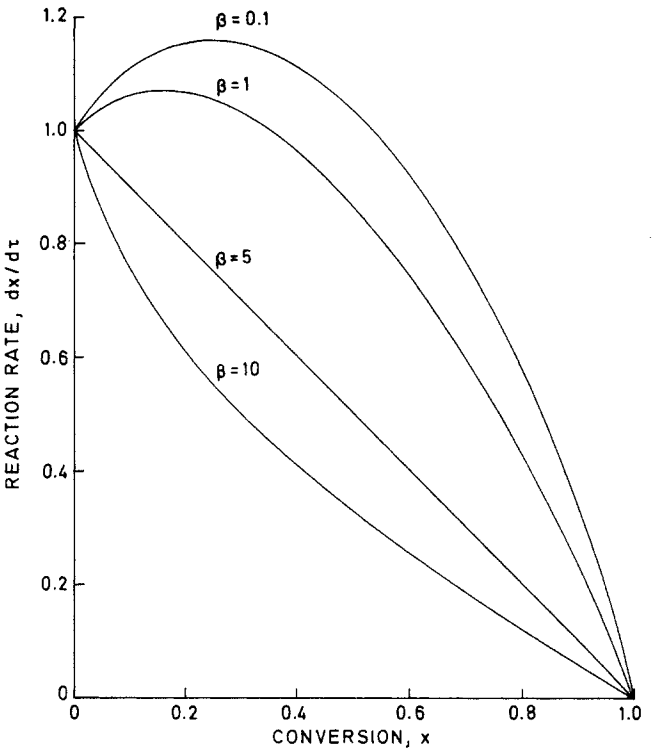

Figure 11. Variation of reaction rate with conversion when intrapellet diffusion is rapid, for various values of β. Parameters are: $\phi = 0$, $Sh = \infty$, $\psi = 5$, $Z = 1$.

The same relationship holds as well locally at any radial position in the particle in the presence of diffusional gradients. However, changes in reaction surface area will initially be more rapid in the neighborhood of the particle outer boundary where the concentration of reactant fluid is highest. As the reactant B near the surface is exhausted the reaction, and hence change in reaction surface, is more rapid in the interior. This effect is shown in Figure 9 which illustrates computed reaction surface-conversion profiles at various times.

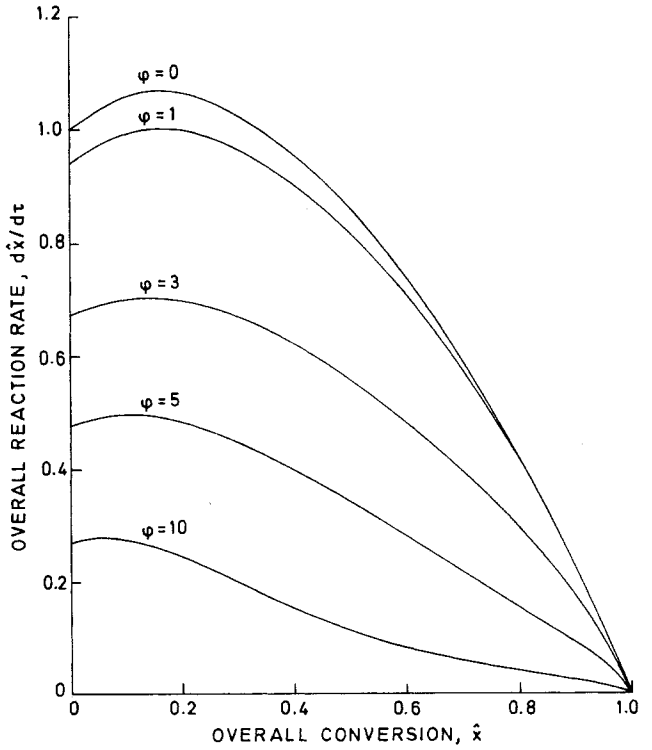

Figure 12. Variation of overall reaction rate with overall conversion, for various values of the Thiele Modulus. Parameters are: $Sh = \infty$, $\psi = 5$, $\beta = Z = 1$.

As anticipated from Eq. 31 for $\psi = 5$ the local reaction surface at any position shows a maximum $(S/S_o) = 1.17$ as conversion proceeds, and according to the Equation the local conversion is 0.26 when this occurs. The value $(S/S_o) = 1.17$ also corresponds to the maximum value in the reaction surface profile; occurring at that radial position at which the local conversion is 0.26. Such effects are apparent in the graphical results presented in Figure 9.

Kawahata and Walker (1962) in their study of the activation of anthracite, observed that the surface area at any given conversion decreased with increase in temperature. Eq. 31 indicates that in the kinetic regime the surface area developed is independent of temperature, so that the observations of Kawahata and Walker (1962) may very likely be due to diffusional effects. To test such a possibility Eqs. 21 to 26 were solved for the case of pure gasification ($Z = 0$), and the relative overall surface area, at any given overall conversion, calculated from:

$$\hat{S} = 3\int_0^1 \left(\frac{S}{S_o}\right)\eta^2 d\eta \tag{32}$$

To introduce the effect of temperature into Eqs. 21-26 the dimensionless variables τ, and ϕ, were referred to their values at a temperature T_1. It was assumed that the fluid obeyed the ideal gas law, and the initial effective diffusivity varied with temperature according to the relation:

$$\frac{(D_{eo})_T}{(D_{eo})_{T_1}} = \left(\frac{T}{T_1}\right)^{\alpha} \tag{33}$$

where the parameter α generally lies between 0.5 and 1.5. Further it was assumed that:

$$\frac{k_s(T)}{k_s(T_1)} = e^{\frac{E}{RT_1}\left(1 - \frac{T_1}{T}\right)} \tag{34}$$

The activation energy was set at 184 MJ/kmol and the reference temperature T_1 at 1000K for the computations. In addition α was chosen to be 1.5. Figure 10 shows the development of the overall surface with change in overall conversion, for various values of the ratio T_1/T. In qualitative agreement with the experimental results of Kawahata and Walker (1962), the overall surface at any conversion is lowered by an increase in temperature. It should be noted here that the parameters used in this computation were arbitrary and not chosen from the data of Kawahata and Walker. Their anthracite coal had a large closed porosity, a feature not accounted for in the formulation developed here.

Reaction Rate

The relationship between the shape parameter of the grain models, and the pore structure parameter of this random-pore model was developed for the kinetic regime in Part I. When product layer diffusion plays a significant role, relations such as Eq. 22 have been derived (Szekely et al., 1976) only for idealized grain shapes with characteristic values of m. In the model presented here Eq. 22 allows the evaluation of reaction rate for any arbitrary ψ, and hence m, when product layer diffusion is included. For example, for $\psi = 0$, Eq. 22 results in:

$$\frac{dX}{d\tau} = \frac{C^*(1 - X)}{1 + \frac{\beta Z}{2} \ln\left(\frac{1}{1 - X}\right)} \tag{35}$$

This is the diffusion corrected form of the first order volume reaction model ($m = 1$) of Ishida and Wen (1971) which, in the kinetic regime, corresponds with $\psi = 0$ (Bhatia and Perlmutter, 1980).

When intrapellet diffusion is rapid, so that concentration gradients are negligible, Eq. 22 expresses the overall reaction rate for the entire particle. In the regime of reaction control (i.e., $\beta = 0$) Eq. 1 predicts the rate maximum as occurring at a conversion of 26%. In the presence of a significant diffusional resistance in the product layer, however, the position of the rate maximum is modified, depending upon the value of β. Figure 11 shows the effect of the product layer diffusion parameter β on the reaction rate when $\psi = 5$, and $\phi = 0$. At $\beta = 0.1$ the change from $\beta = 0$ is only marginal, but by $\beta = 1$ the position has dropped to about 11%.

In fact, for values of β greater than 5 the curves are concave upward, in contrast to the results for kinetic control (Bhatia and Perlmutter, 1980) where the rate versus conversion curve is always convex. The effect of β on the reaction rate is due solely to the concentration gradient in the product layer, because the reaction surface is still related to the conversion by Eq. 31, which is also the result for reaction control.

Figure 12 shows the effect with $\beta = 1$ of the intrapellet diffusional resistance on the overall reaction rate, in terms of the initial Thiele modulus ϕ. The overall rate was obtained by integrating the local reaction rate in Eq. 22:

$$\frac{d\hat{X}}{d\tau} = 3\int_0^1 \frac{dX}{dt}\,\eta^2 d\eta \tag{36}$$

With increase in ϕ the reaction is attenuated, and the position of the rate maximum moved to lower conversions. The change in the position of the rate maximum is, however, not rapid and between $\phi = 0$ and $\phi = 10$, the position changes from about 17% to about 6% on the conversion scale.

As ϕ increases the convexities of the rate versus conversion curves change, and at $\phi = 10$ the curve is concave upward for a short period. This effect which is due to the increasing contribution of intrapellet diffusion to the overall resistance is also evident in Figure 13, which shows the effect of ψ on the overall rate. This dependence on ψ arises from the decrease in the effective relative contribution of product layer diffusion with increasing ψ, expressed in Eq. 22 by the (β/ψ) ratio. At higher conversions, however, when the concentration profile is relatively flat, the

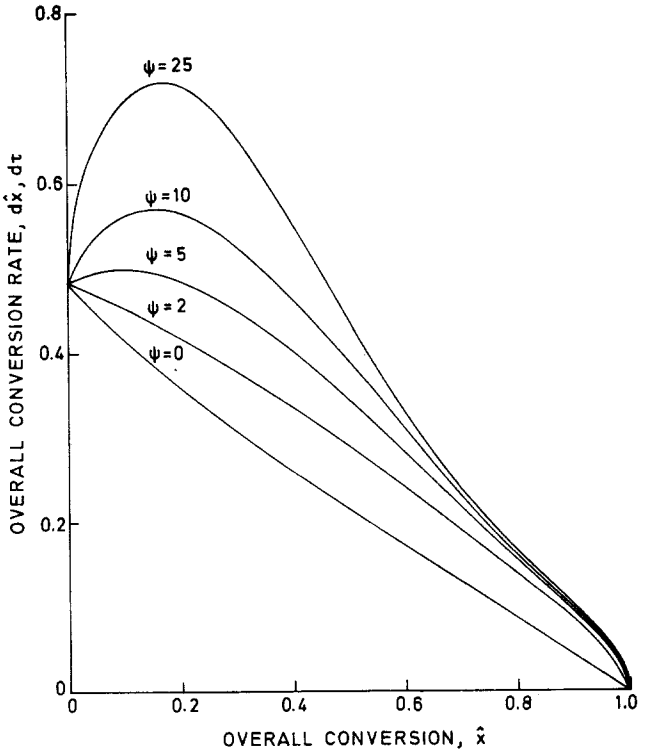

Figure 13. Effect of the pore structure parameter on the overall reaction rate. Parameters are: $\phi = 5$, $Sh = \infty$, $\beta = Z = 1$.

influence of intrapellet diffusion is smaller and the concavity disappears. This behavior of the reaction rate has been reported in several experimental studies. The data of Takamura et al. (1974) on the oxidation of zinc sulfide shows the same effect, when reaction temperature is raised.

Optimal Temperature

The results in Figure 7 indicate that when Z is greater than 1 and the initial porosity is too low for complete conversion, an

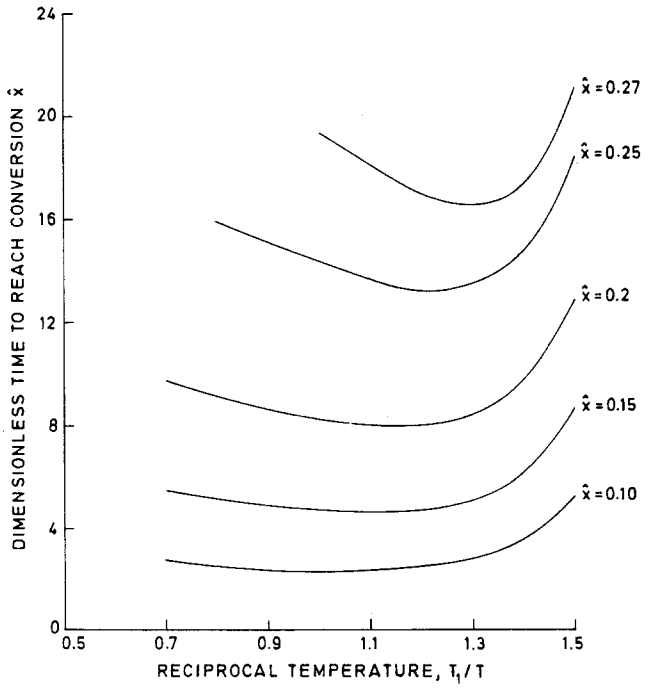

Figure 14. Effect of reaction temperature on time to reach conversion $\hat{X}$. Parameters are: $\phi(T_1) = 15$, $\epsilon_o = 0.5$, $Sh = \infty$, $\psi = 1$, $\beta(T_1) = 75$, $Z = 3.0$, $e^{E/RT1} = 2{,}425$.

increase in the Thiele modulus causes more rapid pore closure at the surface and a decrease in the maximum overall conversion. In such a case an initial increase in reaction rate may occur as reaction temperature is increased, but with the associated increase in the Thiele modulus as diffusional resistance becomes more significant rapid pore closure will decrease the reaction rate. This suggests that an optimal reaction temperature exists at which the time taken to reach a given conversion is a minimum.

Figure 14 shows the results of computations with $Z = 3$, and $\epsilon_o = 0.5$. The dimensionless time to reach a given conversion $\hat{X}$ is referred to its reference value at some fixed temperature T_1. The variation of D_e, and k_s with temperature was assumed to be the same as in Eqs. 33 and 34, with the activation energy set at a value of 73 MJ/kmol, and T_1 at 1120K. The diffusivity in the product layer was assumed to be of the Knudsen type; i.e., D_p was taken as proportional to $[T/T_1]^{0.5}$. In agreement with the above expectation an optimal temperature exists for any conversion $\hat{X}$. For low values of $\hat{X}$ the minimum is not sharply defined, indicating that temperature is not a critical factor if low conversions are desired. With increase in the desired conversion, however, the optimal temperature is better defined and, hence, of greater significance.

Similar optimal temperatures have been reported by Hartman and Coughlin (1976) in their experiments on the sulfation of lime. These authors attributed the optimal temperature to sintering effects by which the temperature was assumed to modify the pore structure. The results of this section indicate that the optimal temperature may be attributed, at least in part, to diffusional effects, when the volume occupied by the product solid is greater than that of the consumed reactant.

ACKNOWLEDGMENT

This research was initially funded by the U.S. Department of Energy, Office of Basic Energy Sciences under Contract No. EY-76-S-02-2747 and completed under National Science Foundation support, Grant No. CPE-8000291.

NOMENCLATURE

a, b = stoichiometric coefficients
C = local concentration of fluid A
C_b = bulk concentration of fluid A
C_i = concentration of A at the reaction surface
C^* = C/C_b
D = diffusion coefficient
D_e = effective diffusivity of fluid A in particle
D_{eo} = initial value of D_e
D_e^* = D_e/D_{eo}
D_p = effective diffusivity of fluid A in product layer
E = activation energy
$f(r)$ = size distribution of nonoverlapped system
k_m = boundary layer mass transfer coefficient
$k_s(T)$ = rate constant for surface reaction at temperature T
L_0 = total length of overlapped system per unit volume, at $t = 0$
m = grain shape factor, or reaction order with respect to solid B
M = molecular weight of solid B
n = reaction order with respect to gas A
p, q = stoichiometric coefficients
r = radius of cylindrical surface
R = radial position
R_o = particle radius
S = reaction surface area per unit volume
$\hat{S}$ = overall reaction surface, per unit volume
S_o = S at $t = 0$
Sh = $k_m R_o/D_{eo}$, modified Sherwood Number
t = time
T = temperature
T_1 = reference temperature
V = volume enclosed by reaction surface, per unit volume of space
V_o = V at $t = 0$
X = local conversion
$\hat{X}$ = overall conversion
Z = ratio of volume of solid phase after reaction to that before reaction

Greek Letters

$\beta = \dfrac{2k_s a\rho(1-\epsilon_o)}{MbD_p S_o}$

Δ = effective thickness of diffusion layer
ϵ = porosity
ϵ_o = ϵ at $t = 0$
ϵ^* = ϵ/ϵ_o
$\gamma(\epsilon)$ = tortuosity
η = R/R_o
$\phi = R_o\sqrt{\dfrac{k_s a\rho S_o}{MbD_{eo}}}$, Thiele Modulus
$\psi = \dfrac{4\pi L_o(1-\epsilon_o)}{S_o^2}$, structural parameter
ρ = mass of solid B per unit volume in original solid phase
τ = $k(T)C_b S_o t/(1-\epsilon_o)$, dimensionless time
τ_1 = τ with k_s, C_b evaluated at $T = T_1$

LITERATURE CITED

Bhatia, S. K., and D. D. Perlmutter, "A Random Pore Model for Fluid-Solid Reactions: I. Isothermal, Kinetic Control," *AIChE J.*, **26**, 379 (1980).

Bischoff, K. B., "Accuracy of the pseudo steady state approximation for moving boundary diffusion problems," *Chem. Eng. Sci.*, **18**, 711 (1963).

Finlayson, B., *The Method of Weighted Residuals and Variational Principles*, Academic Press, London (1972).

Hartman, M., and R. W. Coughlin, "Reaction of Sulfur Dioxide with Limestone and the Grain Model," *AIChE J.*, **22**, 490 (1976).

Ishida, M., and C. Y. Wen, "Comparison of Zone-Reaction Model and Unreacted-Core-Shrinking Model in Solid-Gas Reactions," *Chem. Eng. Sci.*, **26**, 1031 (1971).

Kawahata, M., and P. L. Walker, "Mode of Porosity Development in Activated Anthracite," in *Proceedings of the Fifth Carbon Conference*, **2**, 251-263, Pergamon Press (1962).

Luss, D., "On the Pseudo Steady State Approximation for Gas Solid Reactions," *Can. J. Chem. Eng.*, **46**, 154 (1968).

Petersen, E. E., "Reaction of Porous Solids," *AIChE J.*, **3**, 442 (1957).

Ramachandran, P. A. and J. M. Smith, "A Single-Pore Model for Gas-Solid Non-Catalytic Reactions," *AIChE J.*, **23**, 353 (1977).

Satterfield, C. N., *Mass Transfer in Heterogeneous Catalysis*, M.I.T. Press, Cambridge, Mass. (1970).

Smith, J. M., *Chemical Engineering Kinetics*, McGraw-Hill (1970).

Szekely, J., J. W. Evans, and H. Y. Sohn, *Gas-Solid Reactions*, Academic Press, London (1976).

Takamura et al., "Kinetic Study of Oxidation of Zinc Sulfide Pellets," *J. Chem. Eng. Jap.*, **7**, 276 (1974).

Wakao, N., and J. M. Smith, "Diffusion in Catalyst Pellets," *Chem. Eng. Sci.*, **17**, 825 (1962).

Manuscript received October 1, 1979; revision received July 14, and accepted July 16, 1980.